Distributed Model Predictive Load Frequency Control of multi-area Power Grid: A Decoupling Approach ⋆

Eleftherios E. Vlahakis * **Leonidas D. Dritsas** ** **George D. Halikias** *

* *School of Mathematics, Computer Science and Engineering, City, University of London, UK (e-mail: eleftherios.vlahakis@city.ac.uk, g.halikias@city.ac.uk)*
** *Department of Electrical & Electronic Engineering Educators, School of Pedagogical & Technological Education, ASPETE, Athens, Greece (e-mail: dritsas@aspete.gr)*

Abstract: A model-predictive scheme for load frequency control of a multi-area power system is proposed. The method depends on a decoupling technique which allows for a control design with a distributed architecture. Treating the total power inflows of each area as input variables, a decoupled linearized model for each area is derived. This allows for the formulation and solution of a model predictive control problem with a quadratic performance index and input saturating constraints on the individual tie-line power flows, along with an overall equality constraint to address the energy balance of the network. It is assumed that the interconnection topology (tie-lines) coincides with the communication topology of the network. The only information which needs to be shared between interconnected areas is the local frequency variables. The effectiveness of the method is illustrated via a simulation study of a three-area network. Future work will attempt to establish formally the stability of the control scheme and to enhance the versatility of the method by including constraints on the state variables.

Keywords: distributed model predictive control, load frequency control, automatic generation control, interconnected power system.

1. INTRODUCTION

Power system networks are formed of control areas which are interconnected via transmission lines referred to as tie-lines. Each area is assumed to maintain a single nominal frequency across its geographical region and comprises either a single generator or group of generators. The area is responsible for meeting power demand of its own consumers as well as certain neighboring areas with which the power exchange is normally scheduled for a contracted value. However, due to power load differentiation with the power generation, the frequency of each area along with the scheduled power exchange with its interconnected peers are altered from their nominal value. This violation of the network steady-state operation can be described as a disturbance rejection problem of large-scale interconnected systems with state and input constraints.

Load Frequency Control (LFC) is one of the most challenging problems in multi-area power systems. Textbooks providing an introduction to power systems design and LFC can be found in Bevrani (2010) and Kundur (1994). In typical situations the geographical expanse and the mere complexity of the system resulting from dynamical couplings among the areas make centralized control schemes either impossible or undesirable (Scattolini (2009)). Hence, decentralized and distributed control is typically needed to ensure stable network operation. Analytical methods for designing decentralized and distributed load frequency control have been presented in Siljak et al. (2002); Andreasson et al. (2012); Bidram et al. (2014). A set-theoretic method for LFC design in the context of cyber-physical power systems can be found in Kontouras et al. (2018) while the authors Dritsas et al. (2018) propose LFC design based on an anti-windup compensator assuring stability of the closed-loop system even in cases of large load disturbance. In this work we propose a distributed model predictive based load frequency controller to recover the nominal value of frequency and tie-line power exchange and compensate for unknown step disturbances representing power load demand deviations.

Model predictive control has attracted attention from the power system community in recent years due to its convenience to manage online disturbance rejection problems with state and input constraints, a feature which is highly desired for LFC design. Distributed model predictive based LFC for multi-area interconnected power systems has been presented in Ma et al. (2014). Therein a standard coupled state-space model of each area is employed for state predictions by the MPC scheme where Generation Rate Constraint (GRC) and load reference constraint are considered. Model predictive control with decentralized and distributed structure with application to power systems have been also presented in Mohamed et al. (2011) and Venkat et al. (2008), respectively.

Our method depends on a decoupling technique which allows for a control design with a distributed architecture. Treating the total power inflows of each area as input variables, a decoupled linearized model for each area is derived. This allows for the solution of a model predictive control problem with a quadratic performance index and input saturating constraints on the individual tie-line power flows, along with an overall equality constraint to address

⋆ This work was supported by a City, University of London scholarship held by Eleftherios Vlahakis.

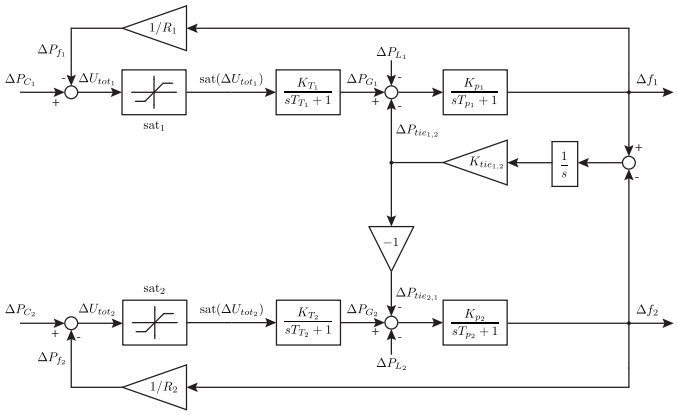

Fig. 1. Block-diagram of two-area power system.

the energy balance of the network. The effectiveness of the method is illustrated via a simulation study of a three-area network.

The remaining of the paper is organized in three sections. In section 2 modelling of two-area power system is presented which is then extended to the multi-area case. Section 3 is devoted to model predictive control design with distributed structure. In the same section a case study of a three-area power system is examined. Section 4 presents the main conclusions of the work where a discussion of the main results and suggestions for future work are provided.

2. MULTI-AREA POWER SYSTEM DESIGN

2.1 Two- area Modelling

We consider a standard linearized model Bevrani (2010) of a two area power system the block diagram of which is depicted in Fig. 1. The analysis provided next will be extended to the multi-area power system design in the following section. Neglecting saturator dynamics the linear state-space model of the two-area system takes the following form:

$$\dot{x} = Ax + B_u u + B_w w,\ x_0 = x(0) \tag{1}$$

where

$$x = [\Delta f_1\ \Delta f_2\ \Delta P_{G1}\ \Delta P_{G2}\ \Delta P_{tie,1}]' \tag{2}$$
$$u = [\Delta P_{C,1}\ \Delta P_{C,2}]' \tag{3}$$
$$w = [\Delta P_{L,1}\ \Delta P_{L,2}]' \tag{4}$$

represent state, input and disturbance vectors, respectively and

$$A = \begin{bmatrix} -\frac{1}{T_{p1}} & 0 & \frac{K_{p1}}{T_{p1}} & 0 & -\frac{K_{p1}}{T_{p1}} \\ 0 & -\frac{1}{T_{p2}} & 0 & \frac{K_{p2}}{T_{p2}} & +\frac{K_{p2}}{T_{p2}} \\ -\frac{K_{t1}}{R_1 T_{t1}} & 0 & -\frac{1}{T_{t1}} & 0 & 0 \\ 0 & -\frac{K_{t2}}{R_2 T_{t2}} & 0 & -\frac{1}{T_{t2}} & 0 \\ K_{tie1,2} & -K_{tie1,2} & 0 & 0 & 0 \end{bmatrix}, \tag{5}$$

$$B_u = \begin{bmatrix} 0 & 0 & \frac{K_{t,1}}{T_{t,1}} & 0 & 0 \\ 0 & 0 & 0 & \frac{K_{t,2}}{T_{t,2}} & 0 \end{bmatrix}', \tag{6}$$

$$B_{w,5} = \begin{bmatrix} -\frac{K_{p,1}}{T_{p,1}} & 0 & 0 & 0 & 0 \\ 0 & -\frac{K_{p,1}}{T_{p,2}} & 0 & 0 & 0 \end{bmatrix}'. \tag{7}$$

Here, the notation Δ indicates deviation from steady-state operation conditions; for $i = 1, 2$, Δf_i is the frequency deviation from the common nominal value and $\Delta P_{G,i}$ is the deviation from equilibrium value of the electrical power generated by the aggregate generating units of each area. The latter is taken equal to the mechanical power produced in the output of the turbines. $\Delta P_{tie,1}$ denotes the total power inflow to the area 1 with dynamics described by

$$\Delta P_{tie,1} = K_{tie,1,2} \int_0^t (\Delta f_1(\tau) - \Delta f_2(\tau)) d\tau, \tag{8}$$

where $K_{tie,1,2} = 2\pi T_{1,2}$ is the synchronization coefficient between areas 1 and 2. Since power inflow to the area 1 corresponds to equal power outflow from area 2, $\Delta P_{tie,2} = -\Delta P_{tie,1}$ is redundant state and is neglected in eq. (1). All parameters involved in (1) along with basic power system terminology are summarized in Table 1. The disturbance signal $\Delta P_{L,i}$ for $i = 1, 2$ denotes time-varying demand of the consumers of the i-th area and corresponds to unknown, piece-wise constant and bounded power load deviations with known upper and lower limits. Here, we study the case where

$$\Delta P_{L,i,\min} \le \Delta P_{L,i} \le \Delta P_{L,i,\max},\ \text{for } i = 1, 2. \tag{9}$$

Table 1.

Parameter,Symbol	Area 2 / Area 1,3	Units
Nominal Frequency, f^o	50/50	H_z
Power Base, $P_{B,i}$	2000/1500	MW
Load Dependency Factor,D_i	16.66/10.50	$\frac{MW}{H_z}$
Speed Droop, R_i	$1.2 \times 10^{-3}/1.3 \times 10^{-3}$	$\frac{H_z}{MW}$
Generator Inertia Gain, H_i	5 /4	s
Turbine Static Gain, $K_{t,i}$	1 /1	$\frac{MW}{MW}$
Turbine Time Constant, $T_{t,i}$	0.3 /0.25	s
Area Static Gain, $K_{p,i}$	0.06 /0.0952	$\frac{H_z}{MW}$
Area Time Constant, $T_{p,i}$	24 /22.8571	s
Tie-line Coefficient, $K_{tie,i}$	1090/1090	$\frac{MW}{H_z}$

The total control signal of the i-th control area is the sum of two components: $\Delta u_{tot,i} = \Delta P_{f,i} + \Delta P_{C,i}$ namely the primary frequency control action, defined as $\Delta P_{f,i} = -\frac{1}{R_i}\Delta f_i$ and the automatic generation control (AGC) $\Delta P_{C,i}$ to be designed. The first is a fixed static linear control law performed by the speed governor which is a regulating unit attached on the prime mover. Detailed

description of this topic can be found in Kundur (1994). The static gain R_i is commonly referred to as speed droop or speed regulation. The signal $\Delta u_{tot,i}$, $i = 1, 2$ is subjected to a component-wise saturation hard constraint of the form

$$\Delta u_{tot,i,\min} \leq \Delta u_{tot,i} \leq \Delta u_{tot,i,\max}, \ i = 1, 2 \tag{10}$$

where the saturator limits are assumed symmetric in the sense that $\Delta u_{tot,i,\max} = -\Delta u_{tot,i,\min}$. Also, $\Delta u_{tot,i,\max}$ is assumed to be greater than the maximum expected load deviation $\Delta P_{L,i,\max}$ with $i = 1, 2$, otherwise, zero frequency deviation error is not guaranteed. Negative values of $\Delta u_{tot,i,\min}$ allow for handling of negative values of $\Delta P_{L,i}$, that is, in case of load reduction.

Since hard constraints apply to the total input signal of each area it makes sense to formulate the state-space (1) such that $\Delta u_{tot,i}$ appears in the input vector u. This is shown next. Let the AGC signals be written as:

$$\begin{bmatrix} \Delta P_{C,1} \\ \Delta P_{C,2} \end{bmatrix} = \begin{bmatrix} \Delta u_{tot,1} \\ \Delta u_{tot,2} \end{bmatrix} - \begin{bmatrix} \Delta P_{f,1} \\ \Delta P_{f,2} \end{bmatrix} \tag{11}$$

or

$$\begin{bmatrix} \Delta P_{C,1} \\ \Delta P_{C,2} \end{bmatrix} = \begin{bmatrix} \Delta u_{tot,1} \\ \Delta u_{tot,2} \end{bmatrix} + \underbrace{\begin{bmatrix} 1/R_1 & 0 & 0 & 0 & 0 \\ 0 & 1/R_2 & 0 & 0 & 0 \end{bmatrix}}_{B_f} \underbrace{\begin{bmatrix} \Delta f_1 \\ \Delta f_2 \\ \Delta P_{G,1} \\ \Delta P_{G,2} \\ \Delta P_{tie,1} \end{bmatrix}}_{x}. \tag{12}$$

Then adding $B_u B_f x$ to (5) with B_f given in (12), changes the input vector u in (1) to $u = [\Delta u_{tot,1} \ \Delta u_{tot,2}]'$ and eliminates the primary frequency control from the dynamical equation. The matrix (5) is now altered to:

$$A = \begin{bmatrix} -1/T_{p,1} & 0 & K_{p,1}/T_{p,1} & 0 & -K_{p,1}/T_{p,1} \\ 0 & -1/T_{p,2} & 0 & K_{p,2}/T_{p,2} & +K_{p,2}/T_{p,2} \\ 0 & 0 & -1/T_{t,1} & 0 & 0 \\ 0 & 0 & 0 & -1/T_{t,2} & 0 \\ K_{tie,1,2} & -K_{tie,1,2} & 0 & 0 & 0 \end{bmatrix} \tag{13}$$

while matrices B_u and B_w in (6) and (7), respectively, are unaffected. Essentially, once $\Delta u_{tot,i}$ has been designed the AGC signal of each area can be generated by:

$$\Delta P_{C,i} = \Delta u_{tot,i} + \frac{1}{R_i} \Delta f_i \tag{14}$$

since the primary frequency control law $\Delta P_{f,i}$, $i = 1, 2$, is pre-specified.

2.2 State-augmentation for integral action

A well-established technique for tackling step-disturbances with zero steady-state error is to include integral action into the state-space model. For the i-th area consider performance variable expressed as a summation of frequency deviation Δf_i multiplied by a bias factor B_i and tie-line power exchange $\Delta P_{tie,i}$ or $z_i = B_i \Delta f_i + \Delta P_{tie,i}$. This quantity is referred to as Area Control Error (ACE) and a usual choice for B_i is $D_i + \frac{1}{R_i}$, Bevrani (2010). Parameters D_i and R_i are defined in Table 1. Take now $z = [z_1 \ z_2]' = C_z x$ with x given in (2) and

$$C_z = \begin{bmatrix} B_1 & 0 & 0 & 0 & 1 \\ 0 & B_2 & 0 & 0 & -1 \end{bmatrix} \tag{15}$$

and consider the augmented state-vector:

$$x_a(t) = \left[x(t)' \ \int_0^t z_1(\tau) d\tau \ \int_0^t z_2(\tau) d\tau \right]'. \tag{16}$$

Then the augmented state-space form of the two-area power system is written as:

$$\dot{x}_a = A_a x_a + B_{u,a} u + B_{w,a} w \tag{17}$$

with $A_a = \begin{bmatrix} A & 0_{5\times 2} \\ C_z & 0_{2\times 2} \end{bmatrix}$, $B_{u,a} = \begin{bmatrix} B_u \\ 0_{2\times 2} \end{bmatrix}$ and $B_{w,a} = \begin{bmatrix} B_w \\ 0_{2\times 2} \end{bmatrix}$, where A, C_z, B_u and B_w are given in (13), (15), (6) and (7), respectively. Due to state-augmentation by the integral of the ACE signal of each area, designing stabilizing controller u for (17) leads to zero steady-state frequency and tie-line power exchange deviations, provided these are driven by step disturbances $\Delta P_{L,i}$, $i = 1, 2$.

In the following section, we propose an equivalent representation of the state-space form of the two-area system which will allow us to derive a pseudo-decoupled model for each area facilitating the multi-area power system design. This will also prove highly useful for the distributed control design. In the sequel all state-space representations are given in the augmented form.

2.3 Decoupled state-space model and multi-area design

By viewing eq. (1) we remark that the two areas are governed by differential equations of the same structure differing only in parameters. Also the coupling between the dynamics is due to $\Delta P_{tie,1}$ variable pertaining to the power exchange deviation between the two areas. By introducing the variable $\Delta P_{tie,2} = -\Delta P_{tie,1}$ defined by

$$\Delta P_{tie,2} = K_{tie,2,1} \int_0^t (\Delta f_2(\tau) - \Delta f_1(\tau)) d\tau, \tag{18}$$

where $K_{tie,2,1} = K_{tie,1,2}$ the state-space form of each area in a two-area system can be written as:

$$\begin{bmatrix} \Delta \dot{f}_i \\ \Delta \dot{P}_{G,i} \\ \Delta \dot{P}_{tie,i} \\ z_i \end{bmatrix} = \begin{bmatrix} -\frac{1}{T_{p,i}} & \frac{K_{p,i}}{T_{p,i}} & -\frac{K_{p,i}}{T_{p,i}} & 0 \\ 0 & -\frac{1}{T_{t,i}} & 0 & 0 \\ K_{tie} & 0 & 0 & 0 \\ B_i & 0 & 1 & 0 \end{bmatrix} \begin{bmatrix} \Delta f_i \\ \Delta P_{G,i} \\ \Delta P_{tie,i} \\ \int z_i d\tau \end{bmatrix} + \begin{bmatrix} 0 \\ 0 \\ -K_{tie} \\ 0 \end{bmatrix} \Delta f_j + \begin{bmatrix} 0 \\ \frac{K_{t,i}}{T_{t,i}} \\ 0 \\ 0 \end{bmatrix} \Delta u_{tot,i} + \begin{bmatrix} -\frac{K_{p,i}}{T_{p,i}} \\ 0 \\ 0 \\ 0 \end{bmatrix} \Delta P_{L,i}, \tag{19}$$

for $i, j = 1, 2$, where $K_{tie} = K_{tie,1,2} = K_{tie,2,1}$.

Consider now multi-area power grid composed of N areas (generically non-identical). These are interconnected through transmission lines referred to as tie-lines the topology of which is modelled by an undirected graph $\mathcal{G} = (\mathcal{V}, \mathcal{E})$ since the power exchange between interconnected areas is considered bidirectional. Node $i \in \mathcal{V}$ represents the i-th interconnected area while $(i, j) \in \mathcal{E}$ stands for the corresponding link between area i and j. We assume that the graph is not necessarily complete which implies that the topology of tie-lines is sparse. The set of areas connected to the i-th node through tie-lines is denoted by $\mathcal{N}_i \subset \mathcal{V}$. Let now $\Delta P_{tie,i}$ represent the total power inflow to the i-th area with dynamics described by

$$\Delta P_{tie,i} = \sum_{j \in \mathcal{N}_i} K_{tie,i,j} \int_0^t (\Delta f_i(\tau) - \Delta f_j(\tau)) d\tau \tag{20}$$

for $i = 1, \cdots, N$. A decoupled state-space equation of the i-th interconnected area can take the following form:

$$\begin{bmatrix}\Delta\dot{f}_i\\ \Delta\dot{P}_{G,i}\\ \dot{z}_i\end{bmatrix}=\underbrace{\begin{bmatrix}-\frac{1}{T_{p,i}} & \frac{K_{p,i}}{T_{p,i}} & 0\\ 0 & -\frac{1}{T_{t,i}} & 0\\ B_i & 0 & 0\end{bmatrix}}_{A_i}\underbrace{\begin{bmatrix}\Delta f_i\\ \Delta P_{G,i}\\ \int z_i d\tau\end{bmatrix}}_{x_i}$$
$$+\underbrace{\begin{bmatrix}0 & -\frac{K_{p,i}}{T_{p,i}}\\ \frac{K_{t,i}}{T_{t,i}} & 0\\ 0 & 1\end{bmatrix}}_{B_{u,i}}\underbrace{\begin{bmatrix}\Delta u_{tot,i}\\ \Delta P_{tie,i}\end{bmatrix}}_{u_i}+\underbrace{\begin{bmatrix}-\frac{K_{p,i}}{T_{p,i}}\\ 0\\ 0\end{bmatrix}}_{B_{wi}}\underbrace{\Delta P_{L,i}}_{w_i} \quad (21)$$

with $\Delta u_{tot,i} = \Delta P_{C,i} + \Delta P_{f,i}$ for $i = 1,\cdots,N$. Note that $\Delta P_{tie,i}$ has been eliminated from the state-vector and instead is included in the input vector of the i-th area. This technical manipulation results in dynamical decoupling of the interconnected areas and will be utilized in the derivation of LFC controllers with distributed architecture. A schematic representation of (21) is shown in Fig. 2. Since $\Delta P_{tie,i}$ is defined by (20) to avoid any dynamical discrepancy in the model of the i-th area the exact value of this pseudo control variable will be fixed by including hard equality constraints in the control design. We note that this decoupling approach which has not been noticed in the context of relevant literature, will provide considerable flexibility in the control design with distributed architecture.

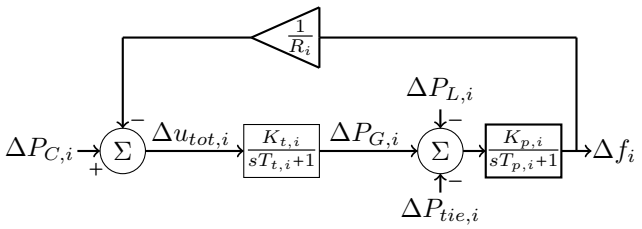

Fig. 2. Single block representation of the i-th interconnected area.

In a multi-area power system the power generation rate of each area should not exceed a specified upper bound. This can be considered as state constraint by the control of each area with typical maximum value for thermal units being $0.0017\ p.u.MW/s$. Comprehensive treatment of this topic can be found in Ma et al. (2014). In this study only input constraints are employed for control design. The control problem examined in this work is stated next.

2.4 Problem statement

Possible power load change in the i-th area of an interconnected power system causes the electrical frequency f_i to deviate from its nominal value. Due to interconnections among the areas through tie-lines and the dependence of the power exchange between the i-th and j-th area upon the difference $\Delta f_i - \Delta f_j$, any power load deviation occurring in the i-th area will affect also the linked j-th area causing transients in its frequency f_j. Here, we formulate the Load Frequency Control of a multi-area power system as disturbance rejection problem with input constraints. We assume that each area can produce LFC signals independently despite the dynamical coupling with certain number of its counterparts, referred to as neighboring areas, with whom it can exchange state information. Effectively, we consider that the topology of physical links (tie-lines) and the topology of information exchange among areas coincide and are described by the same graph. For the problem outlined above, a model predictive controller with distributed architecture is proposed in the following section.

3. LOAD FREQUENCY CONTROL DESIGN

3.1 Model predictive control formulation

Consider multi-area power system of N areas with linearized dynamics described by (21), written here in compact form as:

$$\dot{x}_i = A_i x_i + [B_{u,i}\ B_{w,i}]\begin{bmatrix}u_i\\ w_i\end{bmatrix},\ x_{i,0} = x_i(0), \quad (22)$$

for $i = 1,\cdots,N$. Note that this model is augmented by the ACE signal of each area for integral action purposes. The actual power system evolves in real time while the control subsystem of each area predicts local states within a fictitious future horizon utilizing the system model. For control design, the variables (x_i, u_i, w_i) in (22) are discretized and the predicted discrete-time variables are denoted by $(\hat{x}(\cdot), \hat{u}(\cdot), \hat{w}(\cdot))$. We assume that the local state can be measured while an estimate of the disturbance signal w_i is obtained by appropriate observer.

In our control design the predicted horizon and the control horizon are assumed to be identical and equal to p. The discrete model of the i-th area, obtained as the zero-order-hold equivalent to (22) (continuous-time model), is written as:

$$\begin{aligned}x_i[k+1] &= A_{d,i}x_i[k] + [B_{d,u,i}\ B_{d,w,i}]\begin{bmatrix}u_i[k]\\ w_i[k]\end{bmatrix}\\ x_{i,0} &= x_i[0].\end{aligned} \quad (23)$$

We note here that the hatted variables are not necessarily the same as the actual variables. Hence, $\hat{x}_i[k+p|k]$ is the predicted state of the i-th area after p sampling intervals starting from k and propagating to the future horizon p driven by a sequence of open-loop input functions $\hat{u}_i[k|k],\cdots,\hat{u}_i[k+p-1|k]$. For the i-th area let

$$X_i[k] = \Phi_i x_i[k] + \Psi_{i,1}U_i[k] + \Psi_{i,2}W_i[k] \quad (24)$$

be aggregate vector which stacks p consecutive predicted states from the instant k, with

$$X_i[k] = [\hat{x}_i[k+1|k]'\ \hat{x}_i[k+2|k]'\ \cdots\ \hat{x}_i[k+p|k]']', \quad (25)$$
$$U_i[k] = [\hat{u}_i[k|k]'\ \hat{u}_i[k+1|k]'\ \cdots\ \hat{u}_i[k+p-1|k]']', \quad (26)$$
$$W_i[k] = [\hat{w}_i[k|k]'\ \hat{w}_i[k+1|k]'\ \cdots\ \hat{w}_i[k+p-1|k]']', \quad (27)$$
$$\Phi_i = \left[A_{d,i}'\ {A_{d,i}^2}'\ \cdots\ {A_{d,i}^p}'\right]', \quad (28)$$
$$\Psi_{i,1} = \begin{bmatrix}B_{d,u,i} & 0 & \cdots & 0\\ A_{d,i}B_{d,u,i} & B_{d,u,i} & \cdots & 0\\ \vdots & \vdots & \ddots & \vdots\\ A_{d,i}^{p-1}B_{d,u,i} & A_{d,i}^{p-2}B_{d,u,i} & \cdots & B_{d,u,i}\end{bmatrix}, \quad (29)$$
$$\Psi_{i,2} = \begin{bmatrix}B_{d,w,i} & 0 & \cdots & 0\\ A_{d,i}B_{d,w,i} & B_{d,w,i} & \cdots & 0\\ \vdots & \vdots & \ddots & \vdots\\ A_{d,i}^{p-1}B_{d,w,i} & A_{d,i}^{p-2}B_{d,w,i} & \cdots & B_{d,w,i}\end{bmatrix}. \quad (30)$$

Essentially, the vector $X_i[k]$ contains all the state predictions over the future horizon p. These are computed by the controller which employs the actual state $x_i[k]$ to initialize the prediction. In the extreme case where the actual value $x_i[k]$ is not available at the k-th instant, the controller may perform the prediction starting from the last available predicted state, e.g. $\hat{x}_i[k|k-1]$.

The constrained optimal control problem for each area $i = 1, \cdots, N$ at time instant k is formulated as:

$$\min_{U_i[k]} \; J(x_i[k], U_i[k]) \tag{31}$$

with

$$J(x_i[k], U_i[k]) = X_i[k]' \tilde{Q}_i X_i + U_i[k]' \tilde{R}_i U_i[k] \tag{32}$$

subject to:

$$X_i[k] = \Phi_i x_i[k] + \Psi_{i,1} U_i[k] + \Psi_{i,2} W_i[k] \tag{33}$$

$$[I_p \otimes [0 \;\; 1]] \, U_i[k] = \begin{bmatrix} \Delta P_{tie,i}[k] \\ \Delta \hat{P}_{tie,i}[k+1|k-1] \\ \vdots \\ \Delta \hat{P}_{tie,i}[k+p-1|k-1] \end{bmatrix} \tag{34}$$

$$\begin{bmatrix} I_p \otimes [1 \;\; 0] \\ -I_p \otimes [1 \;\; 0] \end{bmatrix} U_i[k] < \begin{bmatrix} I_p \otimes \gamma_i \\ I_p \otimes \gamma_i \end{bmatrix} \tag{35}$$

where $\tilde{Q}_i = I_p \otimes Q_i$, $\tilde{R}_i = I_p \otimes R_i$ and $\gamma_i = |\Delta u_{tot,i,max}| = |\Delta u_{tot,i,min}|$. $Q_i = Q_i' \geq 0$ and $R_i = R_i' > 0$ weigh predicted states and inputs, respectively, at each iteration of the predicted horizon. They are tuning parameters of the MPC controller the choice of which can be guided by simulations. The parameter γ_i in (35) represents saturation hard constraint of each area.

Note that the first equality constraint (referring to first instant of the prediction horizon) in (34) is given by the actual value of $\Delta P_{tie,i}[k]$ which is a known signal at instant k. This can be either measured directly or computed as:

$$\Delta P_{tie,i}[k] = \Delta P_{tie,i}[k-1] + t_s \sum_{j \in \mathcal{N}_i} K_{tie,i,j} (\Delta f_i[k-1] - \Delta f_j[k-1]) \tag{36}$$

with t_s representing the sampling period of the discretization. Also, $\Delta P_{tie,i}[k-1]$, $\Delta f_i[k-1]$ and $\Delta f_j[k-1]$ are actual and known signals at the k-th time instant by the i-th controller. Note that the difference equation (36) can be considered as the zero-order-hold equivalent to the continuous model (20). This implies that the proposed MPC controller does not violate the dynamics of the actual model while performs state predictions depending on actual values at the k-th instant. The remaining equality constraints in (34) referring to the following $p-1$ instants of the prediction can be produced by the last available predicted states as shown below:

$$\Delta \hat{P}_{tie,i}[k+1+\mu|k-1] = \Delta \hat{P}_{tie,i}[k+\mu|k-1] + t_s \sum_{j \in \mathcal{N}_i} K_{tie,i,j} (\Delta \hat{f}_i[k+\mu|k-1] - \Delta \hat{f}_j[k+\mu|k-1]) \tag{37}$$

with $\mu = 0, \cdots, p-1$.

In the above quadratic program the finite prediction horizon p was selected identical to the control horizon. We assume that at each iteration k the controller of the i-th area measures the local state $x_i[k]$ and estimates the disturbance signal $w_i[k]$. At the same time it receives the current and the predicted states from its neighboring areas. Also it transmits its own local information (current and predicted states) to them. The distributed model predicted controller for a multi-area interconnected power system can be designed by the following algorithm.

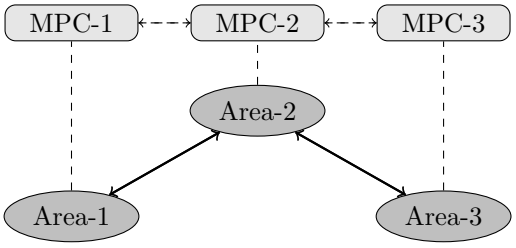

Fig. 3. Topology of physical links (tie-lines) and communication scheme.

Algorithm 1.

1: **Measurement:** Measure $x_i[k]$ and estimate $w_i[k]$.
2: **State Transmission:** Send $x_i[k]$ and $X_i[k-1]$ to neighboring controllers and receive respective information from neighboring areas, $x_j[k]$, $X_j[k-1]$, $j \in \mathcal{N}_i$.
3: **Initialization:** Initialize state prediction starting from $x_i[k]$.
4: **Optimization:** Solve quadratic program (31).
5: **Assignment:** If (31) is feasible: $u_{tot,i}[k] = [1 \;\; 0_{p-1}] \, U_i[k]$, otherwise: $u_{tot,i}[k] = \hat{u}_{tot,i}[k-1]$.
6: **Implementation:** Apply AGC signal $\Delta P_{C,i}[k] = u_{tot,i}[k] + \frac{1}{R_i} \Delta f_i[k]$.
7: **Prediction:** Construct $X_i[k]$.
8: **Termination:** set $k = k+1$ and return to 1.

Remark 1. The optimal control problem (31) requires data transmission among coupled areas. This implies that the communication topology should coincide with the physical topology of the power network in order for the model predictive control strategy proposed to be implemented. Yet, interconnected areas only need to exchange their frequency information (actual and future predictions) while variables associated with the remaining state-vector are not communicated. Hence, in sparse networks with limited interconnections, the communication will not be excessive.

We also wish to mention that important aspects of MPC control, such as recursive feasibility and convergence of the MPC algorithm, are not discussed here. These represent topics of future work. Also, future research will investigate the effects of model uncertainty in conjunction with more advanced techniques from robust MPC.

3.2 Case study: Conceptual three-area power system

Consider a power system of three control areas which are interconnected via tie-lines. The topology of the network is shown in Fig. 3 where the physical links and the communication topology are represented by thick and dashed lines, respectively. The linearized open-loop dynamics of each area is described by (21) with the parameters of the i-th plant being given in Table 1. Each control area is subjected to unknown piece-wise constant disturbances (power demand deviations from equilibrium operation). One scenario is considered for simulation purposes where disturbances $\Delta P_{L,i}$ for $i = 1, 2, 3$ occur at different instances well-spread out over the simulation interval which is taken as 40 $[sec]$. The disturbance of area 1, $\Delta P_{L,1} = 150$ $[MW]$, appears at the first second of the simulation while those of area 2, $\Delta P_{L,2} = 200$ $[MW]$, and 3, $\Delta P_{L,3} = 150$ $[MW]$, at the 11-th and 21-th second, respectively. The control subsystem of each area implements the MPC Algorithm 1 in order to construct its total control signal $\Delta u_{tot,i}$. Then the signal which drives the LFC controller

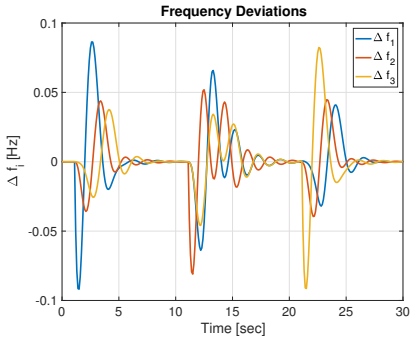

Fig. 4. Frequency deviations of each area driven by step disturbances.

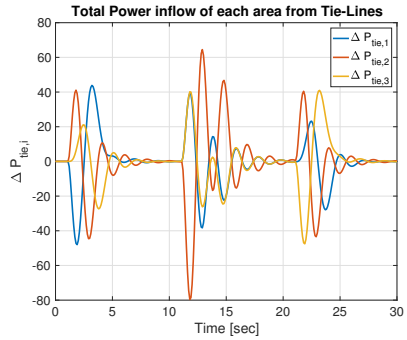

Fig. 5. Power flow via tie-lines.

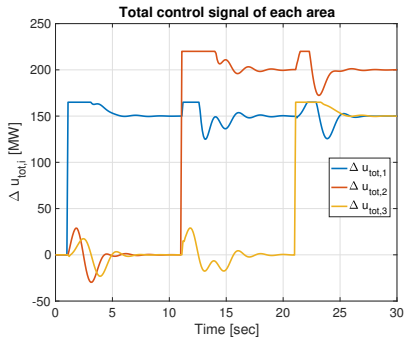

Fig. 6. Total optimal control signal of each area.

$\Delta P_{C,i}$ of each area is derived by (14). The algorithm is performed every $t_s = 0.1$ $[sec]$ using prediction and control horizon $p = 15$. In the simulation the MPC controllers of the three areas have been tuned identically. The choice of the weighting matrices is: $Q_i = \text{diag}(500, 0, 500)$ which penalizes local states and $R_i = 100I_2$ which weighs inputs. The hard constraint γ_i has been taken 10% greater than the magnitude of the respective disturbances of each area.

Fig. 4 and 5 show the transient response of the frequency deviation and the total power-flow deviation from the equilibrium operation of each area. The AGC signal to be constructed at each iteration is given in Fig. 7. This is derived from the optimal control input computed by the MPC controller of each area. This is the total signal which drives the control subsystem of each area and is depicted in Fig. 6. Despite the fact that it is subjected to hard saturation constraints the stable operation of the network is maintained.

4. CONCLUSION

Model predictive load frequency control of a multi-area power system was proposed based on a decoupling technique which allows for control design with distributed

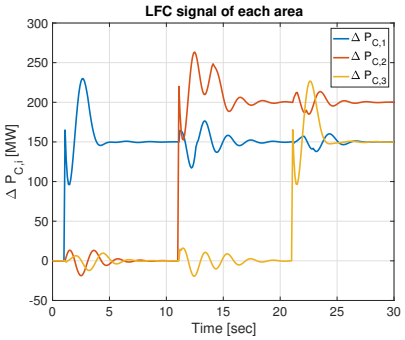

Fig. 7. AGC signal of each area.

architecture. Manipulating the total power inflows to each area as input variables, a decoupled linearized model for each area was derived. This formulation admits of solution to a model predictive control problem with a quadratic performance index and input saturating constraints on the individual tie-line power inflows. An overall equality constraint to address the energy balance of the network was also included in the optimization problem. The only information which the scheme requires be shared between interconnected areas is the local frequency variables. Stability analysis of the control scheme proposed as well as enhancement of the method by including constraints on the state variables will be included in an extended version of this paper.

REFERENCES

Andreasson, M., Sandberg, H., Dimarogonas, D.V., and Johansson, K.H. (2012). Distributed integral action: Stability analysis and frequency control of power systems. In *51st IEEE Conf. Decis. Control*, 2077–2083.

Bevrani, H. (2010). *Robust Power System Frequency Control*.

Bidram, A., Lewis, F.L., and Davoudi, A. (2014). Distributed control systems for small-scale power networks: Using multi-agent cooperative control theory. *IEEE Control Systems*, 34(6), 56–77.

Dritsas, L., Kontouras, E., Kitsios, I., and Tzes, A. (2018). Aggressive Control Design for Electric Power Generation Plants. In *26th Mediterr. Conf. Control Autom.*

Kontouras, E., Tzes, A., and Dritsas, L. (2018). Set-theoretic detection of data corruption attacks on cyber physical power systems. *J. Mod. Power Syst. Clean Energy*, 6(5), 872–886.

Kundur, P.S. (1994). Power system stability. In *Power System Stability and Control*.

Ma, M., Chen, H., Liu, X., and Allgöwer, F. (2014). Distributed model predictive load frequency control of multi-area interconnected power system. *Electr. Power Energy Syst.*, 62, 289–298.

Mohamed, T.H., Bevrani, H., Hassan, A.A., and Hiyama, T. (2011). Decentralized model predictive based load frequency control in an interconnected power system. *Energy Convers. Manag.*

Scattolini, R. (2009). Architectures for distributed and hierarchical Model Predictive Control - A review. *J. Process Control*.

Siljak, D.D., Stipanovic, D.M., and Zecevic, A.I. (2002). Robust Decentralized Turbine/Governor Control Using Linear Matrix Inequalities. *IEEE Power Eng. Rev.*

Venkat, A.N., Hiskens, I.A., Rawlings, J.B., and Wright, S.J. (2008). Distributed MPC strategies with application to power system automatic generation control. *IEEE Trans. Control Syst. Technol.*